

Error Analysis of Option Pricing via Deep PDE Solvers: Empirical Study

Rawin Assabumrungrat
School of Engineering
Tohoku University
Sendai, Japan
rawinassa@gmail.com

Kentaro Minami
Preferred Networks, Inc.
Tokyo, Japan

Masanori Hirano
Preferred Networks, Inc.
Tokyo, Japan
research@mhirano.jp

Abstract—Option pricing, a fundamental problem in finance, often requires solving non-linear partial differential equations (PDEs). When dealing with multi-asset options, such as rainbow options, these PDEs become high-dimensional, leading to challenges posed by the curse of dimensionality. While deep learning-based PDE solvers have recently emerged as scalable solutions to this high-dimensional problem, their empirical and quantitative accuracy remains not well-understood, hindering their real-world applicability. In this study, we aimed to offer actionable insights into the utility of Deep PDE solvers for practical option pricing implementation. Through comparative experiments, we assessed the empirical performance of these solvers in high-dimensional contexts. Our investigation identified three primary sources of errors in Deep PDE solvers: (i) errors inherent in the specifications of the target option and underlying assets, (ii) errors originating from the asset model simulation methods, and (iii) errors stemming from the neural network training. Through ablation studies, we evaluated the individual impact of each error source. Our results indicate that the Deep BSDE method (DBSDE) is superior in performance and exhibits robustness against variations in option specifications. In contrast, some other methods are overly sensitive to option specifications, such as time to expiration. We also find that the performance of these methods improves inversely proportional to the square root of batch size and the number of time steps. This observation can aid in estimating computational resources for achieving desired accuracies with Deep PDE solvers.

Index Terms—High-dimensional PDEs, Deep BSDE methods, Option pricing, Deep PDE solvers

I. INTRODUCTION

Option pricing is a crucial problem in finance. One of the fundamental tools in option pricing is the pricing framework based on risk-neutral measures [1], [2]. The calculation of risk-neutral prices has been frequently formulated as a solution to partial differential equations (PDEs) since the seminal contribution of Black and Scholes (1973) [3]. The requirements of practical finance encompass the valuation of options on multiple underlying assets, such as basket options or credit value adjustments (CVAs), which entail the possibility of high-dimensional PDEs. However, conventional techniques, including finite difference methods and finite element methods, fall prey to the curse of dimensionality, posing a challenge to their scalability to high-dimensional PDEs. Therefore, attention has recently been focused on new PDE solvers that can scale to high dimensions [4].

Deep BSDE solver ([5], [6]) is a promising high-dimensional PDE solver based on deep learning, which solves the equivalent backward stochastic differential equation (BSDE) of the PDE to be solved by optimizing the function modeled by a neural network. See [4], [7]–[9] for comprehensive reviews of deep PDE/BSDE solvers and their variants.

Practical option pricing demands a high level of accuracy. However, the current challenge of deep PDE/BSDE solvers is the lack of quantitative accuracy guarantees to achieve the required precision. One reason for this is that current neural network-based function approximation methods commonly incorporate many heuristics, and thus practitioners utilize them as black-box methods. To date, several researchers have investigated the theoretical approximation accuracy of deep learning-based PDE solvers ([10], [11]). Nevertheless, the existing theoretical analyses are mainly centered on the existence of neural networks that approximate solutions. As such, conducting empirical research is imperative to gain a comprehensive understanding of the accuracy of deep PDE methods with practical implementations of neural network models and algorithms.

Our primary objective is to provide practical guidelines for the design of models and training algorithms in option pricing using Deep PDE/BSDE solvers. To this end, it is essential to deeply understand the errors in these methods. There can be multiple sources of errors, including (i) uncertainties inherent in options and their underlying assets, such as high volatility or long maturity, (ii) errors related to asset models, such as discretization errors in simulations, and (iii) optimization errors related to the choice of neural network architectures and optimization algorithms. We elaborate on these issues in section III.

In this paper, we empirically investigate the performance of Deep PDE/BSDE solvers in high-dimensional option pricing. In our experiments in section IV, we examine the performance of existing Deep PDE solvers for pricing high-dimensional rainbow options and discuss the influence of each source of error. Notably, our results demonstrate that the Deep BSDE method [5], [6] consistently outperforms comparative methods, showcasing a consistent robustness to fluctuating option parameters, e.g., time to expiration. Additionally, performance metrics for these methods appear to improve in inverse pro-

portion to the square root of the batch size (proportion to $1/\sqrt{\text{batch size}}$) and the number of time discretization steps (proportion to $1/\sqrt{\text{time steps}}$), which might be useful for computational budgeting for achieving accuracy required for financial applications.

II. BACKGROUND

A. Option pricing via PDE and BSDE

Here, we will review the basics of option pricing using PDEs. We will omit a comprehensive and mathematically rigorous formulation as it is beyond the scope of this paper. See e.g. [1] for an introduction to this topic.

An option price is often formulated as a conditional expectation with respect to a stochastic process. Let X_t ($t \geq 0$) be a d -dimensional process of the underlying asset prices. The asset price dynamics is typically modeled by a stochastic differential equation (SDE)

$$dX_t = \mu(t, X_t)dt + \sigma(t, X_t)dW_t, \quad (1)$$

where W_t is a d -dimensional Wiener process, μ is an \mathbb{R}^d -valued function, and σ is a $d \times d$ matrix-valued function. More precisely, we consider the dynamics of X_t under the risk-neutral measure, where the expected returns of the risky assets are adjusted to match the risk-free rate r . We are interested in pricing an option with maturity $T > 0$. The payoff of the option depends on the price process X_t . For example, a European-type option has a payoff $\phi(X_T)$ that depends on the terminal value of the underlying assets. Given an initial condition $X_t = x$, the price of the option at time t is given as a conditional expectation $u(t, x) = \mathbb{E}[\exp(-r(T-t))\phi(X_T) | X_t = x]$.

The option price $u(t, x)$ can be linked to a PDE as follows. Let \mathcal{L} be a second-order differential operator defined as

$$\mathcal{L} = \sum_i \mu_i(t, x) \frac{\partial}{\partial x_i} + \frac{1}{2} \sum_{i,j} [\sigma \sigma^T]_{i,j}(t, x) \frac{\partial^2}{\partial x_i \partial x_j}.$$

Then, by the Feynman–Kac formula, $u(t, x)$ solves the Black–Scholes PDE [3]

$$\frac{\partial}{\partial t} u(t, x) + \mathcal{L}u(t, x) = ru(t, x), \quad t \in [0, T], x \in \mathbb{R}^d$$

with a terminal condition $u(T, x) = \phi(x)$, $x \in \mathbb{R}^d$. For more intricate options (e.g., exotics), the payoff can depend on the entire trajectory of X_t , but their prices can still be formulated as solutions of PDEs (see, e.g., [1, Chap. 7]). More generally, this formulation can be extended to a parabolic PDE

$$\frac{\partial}{\partial t} u(t, x) + \mathcal{L}u(t, x) = f(t, x, u(t, x), \sigma^\top(t, x) \nabla_x u(t, x)). \quad (2)$$

with a non-linear contribution term f , which covers a wider range of financial applications, such as xVA computation ([12], [13]) and stochastic control problems.

Furthermore, the solution $u(t, x)$ of (2) can be characterized as a solution of a BSDE [14]. To this end, we define new processes $Y_t = u(t, X_t)$ and $Z_t = \nabla_x u(t, X_t)$, where X_t

follows the (forward) SDE (1) with the initial condition $X_{t_0} = x$. Then, (Y_t, Z_t) satisfies the following BSDE

$$Y_t = \phi(X_T) - \int_t^T f(s, X_s, Y_s, Z_s)ds - \int_t^T Z_s \cdot dW_s \quad (3)$$

for $t_0 \leq t \leq T$. Conversely, if (Y_t, Z_t) solves (3), then $Y_{t_0} = u(t_0, x)$ becomes a (viscosity) solution of the PDE (2). This observation forms the crux of Deep BSDE methods discussed in the following subsection.

B. Deep BSDE methods

In recent years, there has been a surge of interest in algorithms that utilize deep learning techniques for approximating solutions of PDEs (see e.g. [7], [15]). The Deep BSDE method, first introduced by [5], [6], leverages the aforementioned correspondence between PDEs and BSDEs to achieve scalability for high-dimensional PDEs. Here, we provide an overview of several variants of the Deep BSDE method. Comprehensive reviews can be found in [4], [7]–[9].

In what follows, we use the following notations. Let $t_0 = 0 < t_1 < \dots < t_N = T$ be a subdivision of the time interval $[0, T]$ and $\Delta t_i := t_{i+1} - t_i$ for $i = 0, 1, \dots, N-1$. We consider the Euler discretization of (1) defined by

$$\hat{X}_{i+1} = \hat{X}_i + \mu(t_i, \hat{X}_i)\Delta t_i + \sigma(t_i, \hat{X}_i)\Delta W_i \quad (4)$$

for $i = 0, 1, \dots, N-1$, where $\hat{X}_0 = X_0$ is the initial value of the original SDE and $\Delta W_i := W_{t_{i+1}} - W_{t_i}$. Note that ΔW_i are independent normal random variables with mean 0 and variance Δt_i , so we can numerically simulate (4). Below, the expectation symbol \mathbb{E} are to be understood as empirical expectations based on simulations of the Euler method.

1) *Deep BSDE method (DBSDE)*: The *Deep BSDE method (DBSDE)* [5], [6], also known as the “forward scheme”, leverages the forward induction representation of the BSDE (3):

$$\begin{aligned} \hat{Y}_{i+1} &= \hat{Y}_{i+1}^{u_0, \hat{Z}} \\ &:= \hat{Y}_i + f(t_i, \hat{X}_i, \hat{Y}_i, \hat{Z}_i(\hat{X}_i))\Delta t_i + \hat{Z}_i(\hat{X}_i) \cdot \Delta W_i. \end{aligned}$$

To ensure that \hat{Y}_N satisfies the terminal condition, we minimize the following objective

$$J(u_0, \{\hat{Z}_i\}_{i=0}^{N-1}) := \mathbb{E} \left| \hat{Y}_N^{u_0, \hat{Z}} - g(\hat{X}_N) \right|^2$$

with respect to the initial value $\hat{Y}_0 = u_0$ and functions $\hat{Z}_i : \mathbb{R}^d \rightarrow \mathbb{R}^d$ ($i = 0, \dots, N-1$), where each \hat{Z}_i is modeled by a neural network. The output of the method is the approximate solution $u_0 = u(0, X_0)$ at time $t = 0$.

2) *Deep Backward Dynamic Programming (DBDP)*: The *Deep Backward Dynamic Programming* [16] is another approach based on the following backward induction scheme

$$\hat{Y}_i = \hat{Y}_{i+1} - f(t_i, \hat{X}_i, \hat{Y}_i, \hat{Z}_i)\Delta t_i - \hat{Z}_i \cdot \Delta W_i.$$

Starting from $U_N = g$, this method trains neural networks $\{U_i\}_{i=0}^{N-1}$ and $\{V_i\}_{i=0}^{N-1}$ to minimize the following objective function

$$J_i(U_i, V_i) := \mathbb{E} \left| U_{i+1}(\widehat{X}_{i+1}) - U_i(\widehat{X}_i) - f(t_i, \widehat{X}_i, U_i(\widehat{X}_i), V_i(\widehat{X}_i))\Delta t_i - V_i(\widehat{X}_i) \cdot \Delta W_i \right|^2$$

sequentially for $i = N - 1, \dots, 0$. Here, $U_i : \mathbb{R}^d \rightarrow \mathbb{R}$ and $V_i : \mathbb{R}^d \rightarrow \mathbb{R}^d$ are unknown functions modeled by neural networks. It should be noted that U_i corresponds to the solution of the original PDE $u(t_i, \cdot)$, while V_i corresponds to its gradient $\sigma^\top(t_i, \cdot) \nabla_x u(t_i, \cdot)$. [16] proposed two variants of the method; *DBDP1* models U_i s and V_i s with independent neural networks. *DBDP2* models U_i s by scalar-valued neural networks, and compute $V_i(\cdot) = \sigma(t_i, \cdot)^\top \nabla_x U_i(\cdot)$ via automatic differentiation.

3) *Deep Splitting method (DS)*: The *Deep Splitting (DS)* method [17] is similar to *DBDP2* in that it is based on the backward induction and it approximates Z_t using automatic differentiation. A key difference is that the DS employs network values $U_{i+1}(\widehat{X}_{i+1})$ of previous time steps in the nonlinearity f :

$$J_i(U_i) := \mathbb{E} \left| U_{i+1}(\widehat{X}_{i+1}) - U_i(\widehat{X}_i) - f(t_i, \widehat{X}_{i+1}, U_{i+1}(\widehat{X}_{i+1}), V_{i+1})\Delta t_i \right|^2$$

where $V_{i+1} := \sigma^\top(t_i, \widehat{X}_i) \nabla_x U_{i+1}(\widehat{X}_{i+1})$ ¹.

4) *Deep Backward Multistep method (MDBDP)*: The *Deep Backward Multistep Method (MDBDP)* [18] relies on the following iterated representation of the backward induction

$$\widehat{Y}_i = g(\widehat{X}_N) - \sum_{j=i}^{N-1} \left[f(t_j, \widehat{X}_j, \widehat{Y}_j, \widehat{Z}_j)\Delta t_j + \widehat{Z}_j \cdot \Delta W_j \right]. \quad (5)$$

For $i = N - 1, \dots, 0$, this method minimizes the objective function

$$J_j(U_j, V_j) := \mathbb{E} \left| g(\widehat{X}_N) - \sum_{i=j+1}^{N-1} \left[f(t_i, \widehat{X}_i, U_i(\widehat{X}_i), V_i(\widehat{X}_i))\Delta t_i + V_i(\widehat{X}_i) \cdot \Delta W_i \right] - U_j(\widehat{X}_j) \right|^2$$

with respect to neural networks $U_i : \mathbb{R}^d \rightarrow \mathbb{R}$ and $V_i : \mathbb{R}^d \rightarrow \mathbb{R}^d$. Thus, the neural network architecture trained in *MDBDP* is similar to that of *DBDP1*, but it is expected that the use of the iterated representation (5) will reduce error propagation.

¹Here, we introduce a slightly modified version of the method introduced by [18], rather than the original definition [17].

III. SOURCE OF ERRORS IN DEEP OPTION PRICING METHODS

This section provides details of the three sources of errors to which Deep PDE/BSDE solvers are subject. Additionally, the behavior of error arising from each source, as well as how it affects the solvers' performance, is explained in order to make clear the limitations of Deep PDE/BSDE solvers. These issues are then empirically illustrated through the experiments detailed in section IV.

A. Errors inherent in options' and underlying assets' uncertainties

Option prices represent the expected present values of their total future cash flows. In general, they are determined by the price of the underlying asset (spot price), the option's exercise price (strike price), time to expiration, risk-free rate of interest, and volatility of the underlying assets. Those factors themselves partly determine the errors caused by uncertainties [19]. This paper examined the errors involved with time to expiration, spot and strike prices, and volatility, which drive the random process X_t .

Time to expiration refers to the time that options come due or expire. The accuracy of the numerical approximation depends on the step sizes used in the time grid. A shorter time to expiration typically requires smaller time steps, leading to a finer grid and potentially more accurate results. In contrast, a longer time can cause a coarse grid and deteriorate accuracy [20]. Additionally, the error of approximation can increase near maturity because of numerical instability. Case in point, the approximation near maturity is subject to degrade due to a non-smooth payoff function [20]. Consequently, when the time to expiration is too small, the near-maturity instability dominates. This instability results in larger pricing errors, so smaller step sizes may also be required.

Spot and strike prices play a key role in the intrinsic value of options. Here, we refer to the ratio of spot price S_0 to strike price K as moneyness M . Moneyness plays a role in the pricing error of the used model. For instance, in the Black–Scholes model, the pricing error may be greater when an option is in or out of money than it is at the money. In particular, the Black–Scholes model underprices an in-the-money option, and vice versa. The model's presumptions might not accurately reflect the dynamics of options whose current spot price is far from theirs, making them prone to uncertainty.

The greater the volatility of the underlying asset, the higher the probability that the underlying price exhibits significant fluctuations. In general, as the volatility rises, the prices of all options on that underlying asset cost higher, causing the probability of the underlying price finishing in the money is higher. On the other hand, higher volatility is also associated with higher uncertainties, which are driving causes of errors in Monte Carlo methods. According to [21], using the Monte Carlo (with Jump-Diffusion) model, pricing appears to be less accurate for high-volatility stocks, particularly in long-maturity options. Since a higher volatility means that the

sample paths can deviate more at each time step, the computed average might not accurately reflect the distribution of underlying price in reality, which in turn jeopardizes accuracy.

B. Errors by asset models

Pricing errors in the underlying asset largely affect determined option prices [22]. This subsection specifies errors caused by the nature of the underlying asset’s price sampling, which is an essential step to solve a PDE/BSDE using the deep learning models investigated in this paper.

Time discretization in asset price sampling contributes to an error. This error is principally contributed by the number of time steps as well as the choice of discretization methods, e.g., the Euler method, the first and second Milstein methods, and the extrapolation method. In this paper, we limit to investigating only equal-time discretization — that is, to define $\Delta t = T/N$ where T is time to maturity and N is the number of time steps. We speculate that the pricing error caused by time discretization abides by $O(1/\sqrt{N})$ [23].

The fact that the batch size is limited underscores how the sampling may not accurately represent the true distribution of the price. The estimate’s standard error is proportional to $1/\sqrt{N}$, where N is the total number of trajectory measurements [23]. Additionally, it has been revealed that Monte Carlo methods can misestimate option prices in comparison to analytic solutions because a simulation model may, for example, underplay the tails of the distribution of $\phi(X_T)$, which are key drivers of price [24].

C. Optimization errors

Optimization errors are intrinsic in the process of optimization itself. No optimization algorithm is guaranteed to find the true optimal solution for all problems, and that includes deep option pricing, which relies extensively on neural network optimization. Nonetheless, carefully choosing the appropriate parameters makes it possible to minimize the occurrence and impact of optimization errors. In this paper, we utilize the neural networks as proposed in [5].

Different algorithms, as reviewed in [18], perform the approximation of PDE solutions differently. Therefore, we can hypothesize certain algorithms’ superiority under certain conditions.

The number of iterations of all the training data is crucial to obtain an accurate solution since an insufficient number can put at risk the accuracy of Deep BSDE/PDE solvers. On the other hand, choosing an unnecessarily large number causes an excessive computational cost. Another issue is that there is no recommendation for epochs required to reach an accurate solution, which also needs to balance with the learning rate used.

IV. NUMERICAL EXPERIMENTS

This section details the three experiments conducted to make empirical illustrations of the three types of errors encountered by Deep PDE/BSDE solvers, as described and analyzed in section III. The contents are divided into two subsections:

section IV-A and section IV-B, where each of the three experiments, corresponding to each type of error, is presented.

A. Setting

The Heston model is adopted in the same way for all algorithms [25]. Here the price of the asset S_t , is determined by a stochastic process [26]

$$dS_t = \mu S_t dt + \sqrt{\nu_t} S_t dW_t^S$$

where ν_t , the instantaneous variance is given by

$$d\nu_t = \kappa(\theta - \nu_t) dt + \xi \sqrt{\nu_t} dW_t^\nu,$$

and W_t^S, W_t^ν are Wiener processes with correlation ρ . In the *standard setting* of this paper, the model parameters are assigned as follows $S_0 = 100$, $r = 0.05$, $T = 1$, $\nu_0 = 0.1$, $\theta = 0.1$, $\rho = 0$, $\kappa = 2$, and $\xi = 0.1$: S_0 , the initial stock price (spot price); r , the risk-free interest rate; T , the time to the option’s expiration; ν_0 , the initial variance; θ , the mean rate, or long-term variance of the price, so as t approaches infinity, the expected value of ν_t approaches θ ; ρ , the correlation of the two Wiener processes; κ , the rate at which ν_t reverts to θ ; ξ , the volatility of volatility, or ‘vol of vol,’ which designates the variance of ν_t . The values of ρ , κ , and ξ are the default parameters of options provided by [25]. It is certain that those parameters satisfy the following condition, ensuring that ν_t is strictly positive: $2\kappa\theta > \xi^2$.

Our standard setting uses a call, best-of option of $N = 20$ underlying assets. That is, the payoff function is defined by

$$\phi(X_T) = \max \left\{ \max_{1 \leq i \leq N} S_i - K, 0 \right\}. \quad (6)$$

Note that K stands for the strike price, hereafter defined as S_0/M , and the standard moneyness M is 1.2.

In addition, regarding the standard hyperparameters applied across all tested algorithms, the neural networks have a total of 4 layers, where each hidden layer has 128 nodes. The batch size used during training is set to 64, while the size of the validation set is 2048. The learning rate is 0.01. The time duration is equally divided into 40 time steps. Additionally, in the forward scheme algorithm DBSDE, a total of 8000 iterations are applied after the acceleration scheme [27]. In the backward scheme, the number of iterations of the initially trained time step is 16000, followed by multiple sets of 3000 iterations for the rest of the time steps.

1) *Errors inherent in options’ and underlying assets’ uncertainties*: To explore the errors of this type, one of the time to expiration T , moneyness M , and mean rate θ is varied from the standard setting. The list of used time to expiration is 3/12, 6/12, 9/12, 12/12 (standard), 15/12, 18/12, 21/12 years. The moneyness values are 0.9, 1, 1.1, 1.2 (the standard), and 1.3. Lastly, the following mean rate values are applied: 0.06, 0.08, 0.10 (standard), 0.12, and 0.14.

2) *Errors by asset models*: In this type of error, the time step division is varied to 5, 10, 20, 40 (standard), and 80 while every interval is maintained equal to each other. Alternatively, the training batch size is adjusted from 4, 16, 64 (standard) to 256.

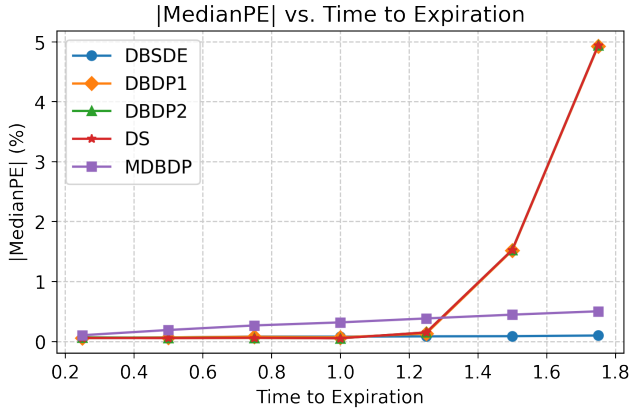


Fig. 1. Experiment 1 (Time to expiration). Both DBSDE and MDBDP exhibit a gradual increase, while DBDP1, DBDP2, and DS demonstrate a rapid ascent. Note that the trajectories of DBDP1, DBDP2, and DS almost overlap.

3) *Optimization errors*: Lastly, we investigate the optimization errors related to the choice of neural network optimization by varying the epochs. In the forward scheme, 125, 500, 2000, 8000 (standard), and 12000 iterations are applied. On the other hand, the first iterations of other backward schemes are modified to 250, 1000, 4000, 16000 (standard), and 24000. In all of the mentioned three experiments, only one of the parameters is adjusted. In other words, all of the other parameters are set to the standard setting.

B. Results

Every single setting described earlier is executed 100 times with all algorithms, and the results are reported in Quartile along with the Monte Carlo solutions. The Monte Carlo solutions are deemed as the accurate representation of true price values. Each Monte Carlo solution is obtained by 10^6 asset price simulations where the time interval is divided into 10^4 steps. The numerical results of all experiments are plotted in Figure 1 to Figure 6, respectively. Every setting in Experiment 1 is paired with a Monte Carlo solution. On the other hand, in Experiments 2 and 3, the Monte Carlo solution is not given because they all represent the standard setting, which has the Monte Carlo option price of 94.933. Besides, either *MedianPE* or *IQR* is reported. MedianPE, or Median Percentage Error, refers to the percentage error of the median in comparison to the Monte Carlo value, whereas IQR refers to the interquartile range – which is calculated by subtracting Q1 from Q3. All factors but batch size have MedianPE as the measurement of error, and its absolute values are plotted in the figures. In the case of batch size, IQR is chosen instead for the fact that the spread of solution distribution rather than its median is influenced by the choice of batch size.

V. DISCUSSION

This section makes empirical analysis and discussion on the obtained results reported in section IV-B. Accordingly, the hypotheses about sources of errors illustrated in section III will be assessed. This section is also divided into four subsections. The first three subsections represent each of the error types:

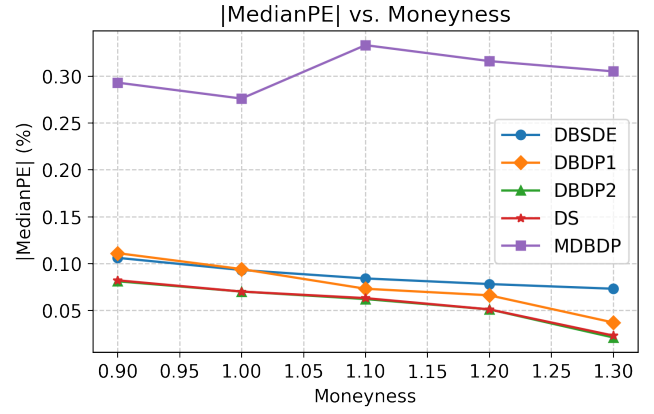


Fig. 2. Experiment 1 (Moneyness). It is obvious that MDBDP produces higher errors than the other algorithms. In this figure, DBDP2 and DS almost overlap.

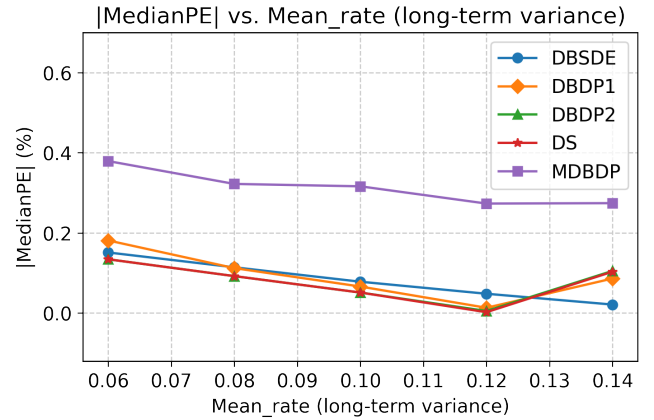


Fig. 3. Experiment 1 (Long-term variance). Similar to fig. 2, MDBDP produces higher errors than the other algorithms, and DBDP2 and DS almost overlap.

options’ and underlying assets’ uncertainties, asset models, and optimization. The last subsection provides a unified comparison among the tested algorithms and our practical guidance on using deep PDE solvers.

A. Errors inherent in options’ and underlying assets’ uncertainties

Regarding time to expiration as in Figure 1, DBDP1, DBDP2, and DS depict not only an increment in error with lengthier times but, notably, glaring errors appear at some points beyond $T = 1.0$. On the other hand, MDBDP and DBSDE demonstrate greater resilience and consistency even as they cause more error when the time to expiration increases, with MDBDP’s error growing faster than DBSDE’s.

In terms of moneyness, the experimental results illustrate that options deeper in the money are associated with less pricing error. DBSDE, DBDP1, DBDP2, and DS all showed a decline in MedianPE as moneyness increases. Throughout the region, DBDP2 produced the lowest error but not significantly lower than DS. By contrast, errors produced by MDBDP were the highest in any tested moneyness, but MDBDP demonstrated a more consistent performance over the studied range.

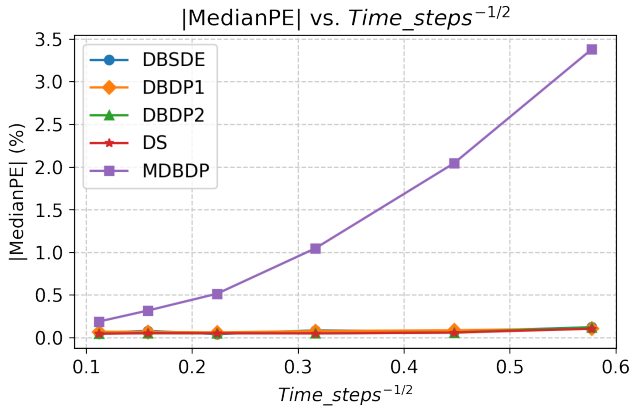


Fig. 4. Experiment 2 (Time steps). MDBDP produces substantially higher errors as the number of time steps decreases (rightward in the graph). Note that all algorithms but MDBDP almost overlap.

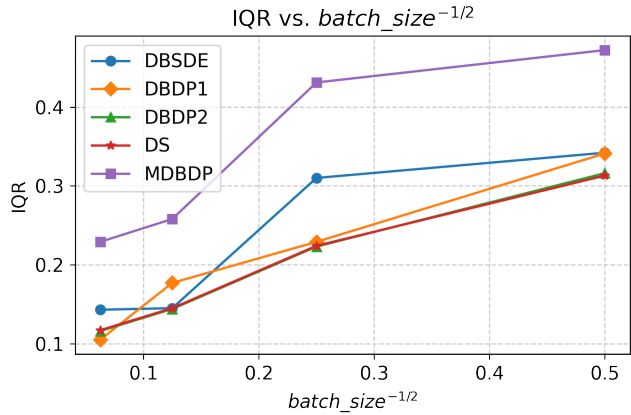


Fig. 5. Experiment 2 (Batch size). Special attention goes to this figure since the measurement of error is the interquartile range not MedianPE.

Its small fluctuation, from 0.276% to 0.333% as shown in Figure 2, is attributed to inexplicable factors.

Generally, as the long-term variance increases, MedianPE shifts downward. Considering the fact that all experiments were run with the initial variance of 0.1, we found that the obtained solutions tend to shift toward the correct prices of options with the final variance of 0.1 because the initial variance was not updated to the defined long-term variance soon enough. In other words, the price of an option where the initial variance was lower than 0.1 was predicted to be higher than its accurate value because its expected variance might not be updated in a timely manner to center around the lower long-term variance. In DBDP2 and DS, the contrary effect happened to be the case: the prices of options where the initial variance was higher than 0.1 were predicted to be lower than their accurate value as their expected variance might not get updated to the higher long-term variance. Nevertheless, the above explanation could not explain the results from DBSDE and MDBDP, and we must attribute the cause of errors in those two algorithms to unexplainable factors.

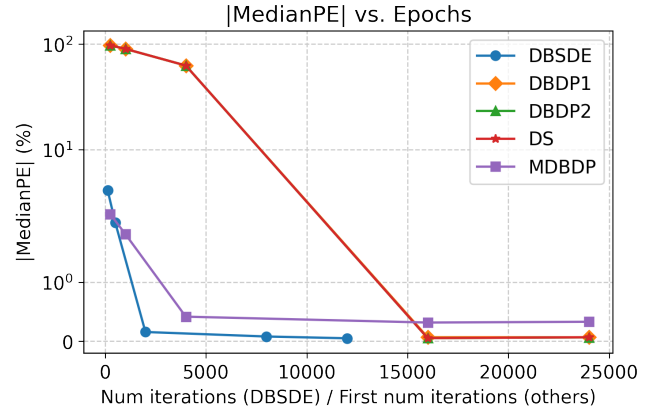


Fig. 6. Experiment 3 (Epochs). This figure incorporates the results from all algorithms for illustration. However, the results from the forward scheme (DBSDE) cannot be compared with those from the backward schemes (others). In case of insufficient epochs, MDBDP's errors are lower than all of the other backward scheme algorithms.

B. Errors by asset models

We examined how changing the number of time intervals and batch sizes affected the final errors. The relationship between $1/\sqrt{\text{batch size}}$ and the results' spread, as determined by the IQR, was clearly proportional for the DBDP1, DBDP2, and DS algorithms. It is firmly illustrated that larger batch sizes produce more consistent results centered around its median. This is consistent with the idea that a small batch size might not fairly reflect the price distribution, which could result in inconsistent estimated option prices. Since there are confirmed advantages to enlarging the batch, it is strongly recommended that batch size in any algorithm is as large as possible. This is especially advised in environments equipped with GPUs where it is unlikely that a larger batch size will hold back computation.

There exists a particularly strong linear relationship between $1/\sqrt{\text{time steps}}$ and error. This confirms our hypothesis that time discretization introduces errors in asset price sampling by suggesting that the error in option pricing tends to decrease as the number of time steps increases. This pattern is most noticeable in MDBDP, where MedianPE escalated by fewer time steps. On the other hand, the other algorithms appear to be affected by other factors, leading to inconsistent and fluctuating outcomes. Besides, although the execution time may not be linearly affected by an increase in the number of time steps, the process may not be as simple as augmenting the batch size. While raising the number of time steps to the greatest extent possible is most preferable, it is recommended to implement at least 20 to 40 time steps, irrespective of the algorithm or time to expiration.

C. Optimization errors

The findings on how the number of iterations affected the accuracy highlight the importance of choosing the right number of iterations. MedianPE strictly decreases as the number of iterations increases. Marked by lowest errors, the best performer was DBSDE, which incorporates the acceleration

scheme [27] in the beginning. One persistent challenge is the absence of a conclusive approach to ascertain the optimal number of iterations, which still requires a trade-off between computational efficiency and solution accuracy. Moreover, the optimal number is subject to a radical change by various factors, e.g., learning rate.

D. Unified comparison

When comparing the performance of different deep PDE solvers in different option pricing scenarios, a significant difference in effectiveness is revealed by changing the specified parameters, particularly the time to expiration and long-term variance. The general ability of DBDP2 and DS to achieve lower MedianPE breaks down when the time to expiration is either too short (≤ 0.25) or too long (≥ 1.25). In these particular cases, DBSDE is the most robust and accurate model, as shown by the MeanPE results in Figure 1. Validated by Figure 3, this resilience of DBSDE further extrapolates to scenarios with high mean variance (≥ 0.14), which seriously compromises the accuracy of DBDP2 and DS, offering DBSDE as a comparative advantage in these conditions.

When this analysis is applied practically, traders must carefully select their algorithms based on particular market conditions and computational limitations. In particular, DBSDE is a strong solution that reduces the errors shown in DBDP2 and DS for options with extended or truncated expiration timelines or those with high mean variance. Additionally, even though MDBDP appears competent, its computational cost is not worthwhile in the financial context where speed is a priority. Therefore, we recommend that the pricing of European-style options with many underlying assets (solving high-dimensional PDEs) should be done with DBSDE. On the other hand, for other option pricing problems where DBSDE cannot be applied, which include but are not limited to pricing American-style options², we suggest that they are solved by MDBDP, which possesses an ability to return the solution path $u(t_i, \cdot)$ at any time step i like other backward schemes.

Regarding our recommendation on settings, it is advisable to always use configurations that at least achieve the best performance within the scope of this paper, especially the batch size, for financial applications where the strictest error reduction measures are crucial. In a real situation, an accurate solution is expected from a single run, and it is necessary to narrow down the spread of an obtained solution. Therefore, we recommend applying the batch size with a minimum of 256 for better consistency and lower variability.

Though these suggestions have a solid empirical basis, it is important to recognize that their applicability is limited to the parameter space that has been studied, which is around the standard parameters in the Heston model. Options with parameters that deviate markedly from our experimental setup might show patterns and behaviors that our current model and comprehension are unable to capture or anticipate. Option

PDEs are subject to additional value adjustment terms (known as xVAs), which would alter our findings to some degree if considered.

VI. CONCLUSION

This paper systematically investigated the error sources in the deep PDE/BSDE solvers on their use in option pricing. Five deep PDE solvers, including DBSDE, DBDP1, DBDP2, DS, and MDBDP, were utilized to solve the Heston PDE and compute the option price in a specified setting. Through a series of devised numerical experiments, insights into errors inherent in options' and underlying assets' uncertainties, asset models, and optimization were empirically explored. The results revealed different advantages of the tested algorithms, and they could confirm relationships between the error and some factors varied in the experiments.

Following the results, we subsequently provided practical advice on how to utilize deep PDE solvers in an efficient manner. In addition, we could solidly reveal the harmful effects of inadequate numbers of time steps, iterations, etc. In addition, we recommended how solvers and settings should be chosen for resilience against inaccuracies. We also discussed the inherent limitations of our experimental environments, which, while informative, do not fully capture the complex nature of options pricing.

REFERENCES

- [1] S. Shreve, *Stochastic Calculus for Finance II: Continuous-Time Models*. Springer New York, 2004.
- [2] N. H. Bingham and R. Kiesel, *Risk-neutral valuation: Pricing and hedging of financial derivatives*. Springer, 2004.
- [3] F. Black and M. Scholes, "The pricing of options and corporate liabilities," *Journal of political economy*, vol. 81, no. 3, pp. 637–654, 1973.
- [4] W. E. J. Han, and A. Jentzen, "Algorithms for solving high dimensional pdes: from nonlinear monte carlo to machine learning," *Nonlinearity*, vol. 35, no. 1, p. 278, dec 2021.
- [5] J. Han, A. Jentzen, and W. E. J. Han, "Solving high-dimensional partial differential equations using deep learning," *The Proceedings of the National Academy of Sciences*, vol. 115, no. 34, pp. 8505–8510, 2018.
- [6] W. E. J. Han, and A. Jentzen, "Deep learning-based numerical methods for high-dimensional parabolic partial differential equations and backward stochastic differential equations," *Communications in Mathematics and Statistics*, vol. 5, pp. 349–380, 2017.
- [7] C. Beck, M. Hutzenthaler, A. Jentzen, and B. Kuckuck, "An overview on deep learning-based approximation methods for partial differential equations," 2020. [Online]. Available: <https://arxiv.org/abs/2012.12348>
- [8] M. Germain, H. Pham, and X. Warin, "Neural networks-based algorithms for stochastic control and PDEs in finance," 2021. [Online]. Available: <https://arxiv.org/abs/2101.08068>
- [9] J. Chessari, R. Kawai, Y. Shinozaki, and T. Yamada, "Numerical methods for backward stochastic differential equations: A survey," *Probability Surveys*, vol. 20, no. none, pp. 486 – 567, 2023. [Online]. Available: <https://doi.org/10.1214/23-PS18>
- [10] P. Grohs, F. Hornung, A. Jentzen, and P. VonWurstemberger, "A proof that artificial neural networks overcome the curse of dimensionality in the numerical approximation of Black-Scholes partial differential equations," *Memoirs of the American Mathematical Society*, 2020.
- [11] M. Hutzenthaler, A. Jentzen, T. Kruse, and T. A. Nguyen, "A proof that rectified deep neural networks overcome the curse of dimensionality in the numerical approximation of semilinear heat equations," *SN Partial Differential Equations and Applications*, vol. 1, no. 10, pp. 1–34, 2020.
- [12] C. Burgard and M. Kjaer, "Partial differential equation representations of derivatives with bilateral counterparty risk and funding costs," *Journal of Credit Risk*, vol. 7, no. 3, pp. 75–93, 2011.

²To explore how (M)DBDP is extended to solve variational inequalities, including the pricing of American-style options, the reader is referred to [16].

- [13] ———, “Funding strategies, funding costs,” *Risk*, vol. 26, no. 12, pp. 82–87, 2013.
- [14] E. Pardoux and S. Peng, “Backward stochastic differential equations and quasilinear parabolic partial differential equations,” in *Stochastic Partial Differential Equations and Their Applications*, B. L. Rozovskii and R. B. Sowers, Eds. Berlin, Heidelberg: Springer Berlin Heidelberg, 1992.
- [15] J. Blechschmidt and O. G. Ernst, “Three ways to solve partial differential equations with neural networks — a review,” *GAMM-Mitteilungen*, vol. 44, no. 2, p. e202100006, 2021.
- [16] C. Huré, H. Pham, and X. Warin, “Deep backward schemes for high-dimensional nonlinear PDEs,” *Mathematics of Computation*, vol. 89, pp. 1547–1579, 2020.
- [17] C. Beck, S. Becker, P. Cheridito, A. Jentzen, and A. Neufeld, “Deep splitting method for parabolic PDEs,” *SIAM Journal on Scientific Computing*, vol. 43, no. 5, pp. A3135–A3154, 2021.
- [18] M. Germain, H. Pham, and X. Warin, “Approximation error analysis of some deep backward schemes for nonlinear pdes,” *SIAM Journal on Scientific Computing*, vol. 44, no. 1, pp. A28–A56, 2022.
- [19] C.-P. Wang, H.-H. Huang, and C.-C. Hung, “Implied index and option pricing errors: Evidence from the Taiwan option market,” *The International Journal of Business and Finance Research*, vol. 5, no. 2, pp. 115–125, 2011.
- [20] O. Pironneau and Y. Achdou, “Partial differential equations for option pricing,” in *Special Volume: Mathematical Modeling and Numerical Methods in Finance*, ser. Handbook of Numerical Analysis, A. Bensoussan and Q. Zhang, Eds. Elsevier, 2009, vol. 15, pp. 369–495. [Online]. Available: <https://www.sciencedirect.com/science/article/pii/S1570865908000112>
- [21] I. Meding and V. Z. Westerlund, “Pricing European options with the Black-Scholes and Monte Carlo methods: a comparative study,” 2022. [Online]. Available: <https://gupea.ub.gu.se/handle/2077/71238>
- [22] L. R. Piccotti, “A closed-form pricing solution for options on assets with pricing errors,” 2021. [Online]. Available: https://papers.ssrn.com/sol3/papers.cfm?abstract_id=3866267
- [23] D.-M. Wang, “Monte Carlo simulations for complex option pricing,” 2011. [Online]. Available: <https://research.manchester.ac.uk/en/studentTheses/monte-carlo-simulations-for-complex-option-pricing>
- [24] P. Godinho, “Monte Carlo estimation of project volatility for real options analysis,” 2006. [Online]. Available: https://papers.ssrn.com/sol3/papers.cfm?abstract_id=926169
- [25] S. L. Heston, “A Closed-Form Solution for Options with Stochastic Volatility with Applications to Bond and Currency Options,” *The Review of Financial Studies*, vol. 6, no. 2, pp. 327–343, 04 2015. [Online]. Available: <https://doi.org/10.1093/rfs/6.2.327>
- [26] P. Wilmott, *Paul Wilmott on Quantitative Finance*. West Sussex, England: Wiley, 2006.
- [27] R. Naito and T. Yamada, “An acceleration scheme for deep learning-based BSDE solver using weak expansions,” *International Journal of Financial Engineering*, vol. 7, no. 2, p. 2050012, 2020.

APPENDIX: COMPLETE TABLES OF THE EXPERIMENTAL RESULTS

In this supplementary material, we provide the complete tables of the experimental results discussed in Section IV. Table I to Table VI correspond to Figure 1 to Figure 6, respectively.

TABLE I
EXPERIMENT 1 (TIME TO EXPIRATION)

Time to expiration	3/12	6/12	9/12	12/12	15/12	18/12	21/12
Monte Carlo	50.857	67.882	82.122	94.933	106.836	118.101	128.883
DBSDE 25%	50.830	67.856	82.100	94.919	106.823	118.096	128.887
DBSDE Median	50.884	67.925	82.187	95.007	106.925	118.203	129.008
DBSDE 75%	50.942	67.989	82.241	95.064	106.999	118.278	129.080
DBSDE MedianPE	0.053%	0.064%	0.079%	0.078%	0.083%	0.086%	0.097%
DBDP1 25%	50.820	67.845	82.079	94.905	106.612	116.235	122.475
DBDP1 Median	50.886	67.926	82.185	94.996	106.698	116.311	122.535
DBDP1 75%	50.937	68.000	82.259	95.082	106.776	116.374	122.580
DBDP1 MedianPE	0.056%	0.065%	0.076%	0.066%	-0.130%	-1.515%	-4.926%
DBDP2 25%	50.845	67.869	82.110	94.929	106.626	116.253	122.494
DBDP2 Median	50.891	67.921	82.171	94.981	106.677	116.299	122.518
DBDP2 75%	50.943	68.002	82.251	95.073	106.784	116.383	122.587
DBDP2 MedianPE	0.066%	0.057%	0.059%	0.051%	-0.149%	-1.526%	-4.938%
DS 25%	50.848	67.871	82.111	94.929	106.627	116.255	122.492
DS Median	50.886	67.919	82.170	94.982	106.677	116.299	122.520
DS 75%	50.944	68.001	82.252	95.074	106.784	116.383	122.591
DS MedianPE	0.057%	0.054%	0.058%	0.051%	-0.149%	-1.525%	-4.937%
MDBDP 25%	50.828	67.930	82.247	95.089	107.087	118.515	129.335
MDBDP Median	50.909	68.010	82.340	95.233	107.245	118.626	129.529
MDBDP 75%	50.970	68.095	82.439	95.347	107.376	118.773	129.700
MDBDP MedianPE	0.102%	0.189%	0.265%	0.316%	0.382%	0.445%	0.501%

TABLE II
EXPERIMENT 1 (MONEYNESS)

Moneyiness	0.9	1	1.1	1.2	1.3
Monte Carlo	68.510	79.079	87.727	94.933	101.030
DBSDE 25%	68.495	79.065	87.713	94.919	101.017
DBSDE Median	68.583	79.153	87.800	95.007	101.105
DBSDE 75%	68.640	79.209	87.858	95.064	101.163
DBSDE MedianPE	0.106%	0.093%	0.084%	0.078%	0.073%
DBDP1 25%	68.476	79.049	87.695	94.905	100.978
DBDP1 Median	68.586	79.153	87.790	94.996	101.068
DBDP1 75%	68.675	79.236	87.890	95.082	101.149
DBDP1 MedianPE	0.111%	0.094%	0.073%	0.066%	0.037%
DBDP2 25%	68.508	79.078	87.725	94.929	101.006
DBDP2 Median	68.565	79.135	87.781	94.981	101.052
DBDP2 75%	68.664	79.233	87.878	95.073	101.144
DBDP2 MedianPE	0.081%	0.070%	0.062%	0.051%	0.021%
DS 25%	68.507	79.076	87.723	94.929	101.005
DS Median	68.566	79.134	87.781	94.982	101.053
DS 75%	68.665	79.234	87.877	95.074	101.144
DS MedianPE	0.082%	0.070%	0.063%	0.051%	0.023%
MDBDP 25%	68.616	79.199	87.907	95.089	101.254
MDBDP Median	68.711	79.297	88.019	95.233	101.338
MDBDP 75%	68.865	79.466	88.104	95.347	101.465
MDBDP MedianPE	0.293%	0.276%	0.333%	0.316%	0.305%

TABLE III
EXPERIMENT 1 (LONG-TERM VARIANCE)

Long-term variance	0.06	0.08	0.10	0.12	0.14
Monte Carlo	84.287	89.717	94.933	99.971	104.857
DBSDE 25%	84.326	89.730	94.919	99.928	104.785
DBSDE Median	84.414	89.819	95.007	100.018	104.879
DBSDE 75%	84.488	89.883	95.064	100.082	104.947
DBSDE MedianPE	0.151%	0.114%	0.078%	0.048%	0.021%
DBDP1 25%	84.327	89.723	94.905	99.891	104.662
DBDP1 Median	84.440	89.818	94.996	99.984	104.767
DBDP1 75%	84.505	89.900	95.082	100.068	104.858
DBDP1 MedianPE	0.181%	0.112%	0.066%	0.013%	-0.086%
DBDP2 25%	84.360	89.750	94.929	99.920	104.701
DBDP2 Median	84.400	89.800	94.981	99.966	104.747
DBDP2 75%	84.490	89.894	95.073	100.064	104.853
DBDP2 MedianPE	0.134%	0.092%	0.051%	-0.005%	-0.105%
DS 25%	84.360	89.750	94.929	99.920	104.701
DS Median	84.399	89.800	94.982	99.969	104.749
DS 75%	84.490	89.895	95.074	100.063	104.851
DS MedianPE	0.134%	0.092%	0.051%	-0.002%	-0.103%
MDBDP 25%	84.508	89.917	95.089	100.133	105.037
MDBDP Median	84.606	90.006	95.233	100.244	105.144
MDBDP 75%	84.714	90.134	95.347	100.356	105.237
MDBDP MedianPE	0.379%	0.322%	0.316%	0.273%	0.274%

TABLE IV
EXPERIMENT 2 (TIME STEPS)

Time steps	3	5	10	20	40	80
DBSDE 25%	94.905	94.908	94.911	94.881	94.919	94.910
DBSDE Median	95.048	94.999	95.013	94.971	95.007	94.985
DBSDE 75%	95.153	95.144	95.102	95.058	95.064	95.070
DBSDE MedianPE	0.121%	0.070%	0.084%	0.040%	0.078%	0.055%
DBDP1 25%	94.942	94.907	94.932	94.906	94.905	94.901
DBDP1 Median	95.034	95.014	95.005	94.989	94.996	94.997
DBDP1 75%	95.110	95.109	95.093	95.071	95.082	95.059
DBDP1 MedianPE	0.107%	0.085%	0.076%	0.060%	0.066%	0.068%
DBDP2 25%	94.979	94.887	94.907	94.900	94.929	94.891
DBDP2 Median	95.046	94.988	94.979	94.980	94.981	94.978
DBDP2 75%	95.120	95.075	95.081	95.051	95.073	95.064
DBDP2 MedianPE	0.120%	0.058%	0.049%	0.049%	0.051%	0.047%
DS 25%	94.958	94.887	94.907	94.900	94.929	94.889
DS Median	95.030	94.988	94.978	94.980	94.982	94.974
DS 75%	95.094	95.075	95.080	95.051	95.074	95.070
DS MedianPE	0.103%	0.058%	0.048%	0.050%	0.051%	0.044%
MDBDP 25%	98.008	96.769	95.828	95.307	95.089	94.993
MDBDP Median	98.141	96.872	95.925	95.421	95.233	95.110
MDBDP 75%	98.320	96.988	96.020	95.556	95.347	95.228
MDBDP MedianPE	3.380%	2.043%	1.045%	0.514%	0.316%	0.187%

TABLE V
EXPERIMENT 2 (BATCH SIZE)

Batch size	4	16	64	256
DBSDE 25%	94.852	94.852	94.919	94.932
DBSDE Median	95.078	95.034	95.007	94.992
DBSDE 75%	95.194	95.162	95.064	95.075
DBSDE IQR	0.342	0.310	0.145	0.143
DBDP1 25%	94.036	94.796	94.905	94.935
DBDP1 Median	94.266	94.914	94.996	94.985
DBDP1 75%	94.378	95.025	95.082	95.039
DBDP1 IQR	0.341	0.229	0.177	0.105
DBDP2 25%	94.038	94.820	94.929	94.942
DBDP2 Median	94.176	94.913	94.981	94.997
DBDP2 75%	94.354	95.042	95.073	95.058
DBDP2 IQR	0.316	0.223	0.144	0.116
DS 25%	94.039	94.819	94.929	94.941
DS Median	94.177	94.914	94.982	94.997
DS 75%	94.352	95.042	95.074	95.058
DS IQR	0.313	0.224	0.145	0.117
MDBDP 25%	94.990	94.985	95.089	95.084
MDBDP Median	95.284	95.211	95.233	95.187
MDBDP 75%	95.462	95.416	95.347	95.312
MDBDP IQR	0.472	0.431	0.258	0.229

TABLE VI
EXPERIMENT 3 (EPOCHS)

Epochs	125	500	2000	8000	12000
DBSDE 25%	98.320	96.543	94.973	94.919	94.901
DBSDE Median	98.866	96.883	95.080	95.007	94.978
DBSDE 75%	99.600	97.419	95.168	95.064	95.097
DBSDE MedianPE	4.143%	2.054%	0.155%	0.078%	0.048%
First-time-step epochs	250	1000	4000	16000	24000
DBDP1 25%	2.368	9.307	35.389	94.905	94.897
DBDP1 Median	2.377	9.318	35.403	94.996	94.994
DBDP1 75%	2.383	9.330	35.414	95.082	95.074
DBDP1 MedianPE	-97.497%	-90.185%	-62.708%	0.066%	0.065%
DBDP2 25%	2.373	9.309	35.396	94.929	94.900
DBDP2 Median	2.376	9.316	35.406	94.981	94.993
DBDP2 75%	2.379	9.324	35.418	95.073	95.116
DBDP2 MedianPE	-97.497%	-90.187%	-62.705%	0.051%	0.064%
DS 25%	2.371	9.309	35.396	94.929	94.900
DS Median	2.376	9.316	35.406	94.982	94.994
DS 75%	2.380	9.323	35.417	95.074	95.116
DS MedianPE	-97.497%	-90.186%	-62.704%	0.051%	0.065%
MDBDP 25%	97.176	95.485	95.217	95.089	95.132
MDBDP Median	97.274	96.664	95.328	95.233	95.245
MDBDP 75%	97.391	97.018	95.448	95.347	95.367
MDBDP MedianPE	2.466%	1.824%	0.416%	0.316%	0.329%

Because forward and backward schemes cannot be compared against each other, the top performers are separately embolden.